

**Journal of Atmospheric and Oceanic Technology**  
**Accuracy and long-term stability assessment of inductive conductivity cell**  
**measurements on Argo floats**  
 --Manuscript Draft--

|  |   |
|--|---|
| <b>Manuscript Number:</b>                  | JTECH-D-20-0058   |
| <b>Full Title:</b>                         | Accuracy and long-term stability assessment of inductive conductivity cell measurements on Argo floats  |
| <b>Article Type:</b>                       | Article   |
| <b>Corresponding Author:</b>               | Nikolay P Nezlin<br>RBR Ltd<br>Anaheim, California UNITED STATES  |
| <b>Corresponding Author's Institution:</b> | RBR Ltd   |
| <b>First Author:</b>                       | Nikolay P Nezlin, Ph.D.   |
| <b>Order of Authors:</b>                   | Nikolay P Nezlin, Ph.D.<br>Mark Halverson, Ph.D.<br>Jean-Michel Leconte<br>Guillaume Maze, Ph.D.<br>Clark Richards, Ph.D.<br>Igor Shkvorets<br>Rui Zhang<br>Greg Johnson, Ph.D.   |
| <b>Abstract:</b>                           | This study demonstrates high levels of long-term stability of salinity measured by Argo floats with inductive conductivity cells, which have extended float lifetimes as compared to electrode-type cells. New Argo float sensor payloads must meet the demands of the Argo governance committees before they are implemented globally. Currently, the use of CTDs with inductive cells, designed and manufactured by RBR Ltd., have been approved as a Global Argo Pilot. One such requirement of new sensors is that they produce stable measurements over the lifetime of a float. To demonstrate this, data from four Argo floats in the western Pacific Ocean equipped with the RBRargo CTD sensor package, are analyzed using the same techniques (OWC method) and reference datasets as the Argo DMQC operators. Being a statistical tool, the OWC method cannot determine whether deviations in the salinity calibration are caused by oceanographic variability or sensor problems. This study demonstrates that anomalous salinity calibration values tend to occur in regions with a high degree of variability and can be explained by imperfect reference data rather than sensor drift. When run with default settings against the standard DMQC Argo and CTD databases, the OWC analysis reveals no drift in any of the four RBRargo datasets and an offset in one case, making the RBR inductive cell a qualified option for salinity measurements in Argo Program. |
| <b>Suggested Reviewers:</b>                | Birgit Klein<br>Federal Maritime and Hydrographic Agency, Germany<br>birgit.klein@bsh.de<br>Argo Steering Team member; Chair of the Euro-Argo ERIC Management Board;<br>Experienced DMQC operator and mentor<br><br>Pelle Robbins<br>Woods Hole Oceanographic Institution, USA<br>probbins@whoi.edu<br>Active member of Argo program<br><br>Peter Oke<br>CSIRO, Australia<br>peter.oke@csiro.au   |



Dear Editor-in-Chief of the “Journal of Atmospheric and Oceanic Technology”,

Thank you for considering our manuscript " Accuracy and long-term stability assessment of inductive conductivity cell measurements on Argo floats" to be published in the “Journal of Atmospheric and Oceanic Technology”. We feel that the subject material is suitable for the Journal. The scope of the paper corresponds to the issues listed among the journal’s focus, including “instrumentation and methods used in atmospheric and oceanic research” and “measurements, validation, and data analysis techniques”.

Our study was designed to evaluate accuracy and stability of Argo drifters equipped with inductive conductivity sensors, a promising energy-saving technology for salinity measurements at autonomous ocean-observing platforms.

On behalf of the authors,

Yours Sincerely

Dr. Nikolay P. Nezlin

1 **Accuracy and long-term stability assessment of inductive**

2 **conductivity cell measurements on Argo floats**

3 **Nikolay P. Nezlin<sup>1\*</sup>, Mark Halverson<sup>1</sup>, Jean-Michel Leconte<sup>1</sup>, Guillaume Maze<sup>2</sup>, Clark**

4 **Richards<sup>3</sup>, Igor Shkvorets<sup>1</sup>, Rui Zhang<sup>1</sup>, and Greg Johnson<sup>1</sup>**

5 *<sup>1</sup>RBR Ltd., Ottawa, ON, Canada*

6 *<sup>2</sup>IFREMER, Brest, France*

7 *<sup>3</sup>Bedford Institute of Oceanography, Dartmouth, NS, Canada*

8 *\*Corresponding author; e-mail: [nikolay.nezlin@rbr-global.com](mailto:nikolay.nezlin@rbr-global.com)*

9

10

## 11 **Abstract**

12 This study demonstrates high levels of long-term stability of salinity measured by Argo floats  
13 with inductive conductivity cells, which have extended float lifetimes as compared to electrode-  
14 type cells. New Argo float sensor payloads must meet the demands of the Argo governance  
15 committees before they are implemented globally. Currently, the use of CTDs with inductive  
16 cells, designed and manufactured by RBR Ltd., have been approved as a Global Argo Pilot. One  
17 such requirement of new sensors is that they produce stable measurements over the lifetime of a  
18 float. To demonstrate this, data from four Argo floats in the western Pacific Ocean equipped  
19 with the *RBRargo* CTD sensor package, are analyzed using the same techniques (OWC method)  
20 and reference datasets as the Argo DMQC operators. Being a statistical tool, the OWC method  
21 cannot determine whether deviations in the salinity calibration are caused by oceanographic  
22 variability or sensor problems. This study demonstrates that anomalous salinity calibration  
23 values tend to occur in regions with a high degree of variability and can be explained by  
24 imperfect reference data rather than sensor drift. When run with default settings against the  
25 standard DMQC Argo and CTD databases, the OWC analysis reveals no drift in any of the four  
26 *RBRargo* datasets and an offset in one case, making the RBR inductive cell a qualified option  
27 for salinity measurements in the Argo Program.

28

## 29 **1. Introduction**

30 The Argo program consists of approximately 4000 autonomous profiling floats continuously  
31 operating in the world ocean (Jayne et al. 2017; Roemmich et al. 2019). Its implementation

32 started in 1999 and it has been providing global coverage of the upper 2000 m of the open ocean  
33 since 2006. More recently, Argo coverage has grown to include seasonal ice zones and marginal  
34 seas. Argo is a part of the Global Ocean Observing System, providing basic oceanographic  
35 information for process studies, ocean model data assimilation, validation, reanalysis and  
36 forecasting (Legler et al. 2015).

37 Data quality is a key asset of the Argo program: target accuracies for measurements are set to 2.5  
38 dbar for pressure, 0.005°C for temperature, and 0.01 for salinity (Riser et al. 2016). The main  
39 obstacle in achieving this goal is that autonomous floats cannot be recalibrated on a regular basis  
40 and, as such, indirect methods of data quality analysis and correction must be applied to achieve  
41 accurate results. For Argo data, quality control includes two steps following the Argo data  
42 collection and dissemination strategy. First, Real Time Quality Control (RTQC) procedures are  
43 applied to the data collected by the floats, focusing on the detection and elimination of outliers  
44 (Udaya Bhaskar et al. 2013; Wedd et al. 2015; Wong et al. 2020). This data is generally made  
45 freely available in Near-Real Time (NRT), that is within 24 h. Second, a Delayed-Mode Quality  
46 Controlled (DMQC) analysis is conducted to produce high quality datasets suitable for  
47 oceanographic research. Delayed-Mode (DM) analysis relies on Argo data experts to examine  
48 the data and apply corrections when necessary. DM products are available to users 6 to 12  
49 months after collection.

50 While temperature and pressure are generally measured within the required accuracies  
51 throughout the life of a float, salinity (computed from conductivity measurements) is more  
52 problematic for two main reasons. First, biofilms can form on the conductivity cell, causing a  
53 change in the cell constant. Mitigation strategies, such as poisoning the water within the cell with

54 tributyltin oxide (TBTO) may reduce biofouling, but TBTO is known to coat the electrodes inside  
55 the conductivity cell for the first few months of a deployment, before eventually washing off  
56 (Wong et al. 2020). Second, mechanical failures can seriously impact measured conductivity.  
57 Recently, for example, large batches of Conductivity-Temperature-Depth (CTD) instruments  
58 SBE41CP from Sea-Bird Scientific (SBE) have been found by DMQC operators and others to  
59 drift salty, potentially arising from the failure of the encapsulant used in the cell construction  
60 (see Argo Steering Team 2018; Section 8). As a result, an essential part of DMQC process is the  
61 analysis and correction of salinity offset and drift using the standard ‘Owens-Wong-Cabanes’  
62 (OWC) method (Cabanes et al. 2016; Owens and Wong 2009).

63 Salinity measurements in the ocean are commonly made using either electrode or inductive  
64 conductometry principles. While electrode cells measure electrical resistance between the  
65 electrodes in direct contact with seawater, inductive cells function according to Faraday’s law of  
66 induction (Halverson et al. 2020). An electrical signal applied to the generating coil produces a  
67 magnetic flux, a resultant electric field, and finally an electromagnetic current induced in the  
68 seawater present in the center of the cell. This current flowing through the receiving coil is  
69 proportional to the resistance of the water, which is inversely proportional to conductivity. The  
70 measured conductivity is transformed to practical salinity using the seawater equation of state  
71 (Fofonoff 1985; McDougall and Barker 2011). Inductive conductivity cells possess key features  
72 that are particularly beneficial for autonomous observing systems (Halverson et al. 2020;  
73 Shkvoretz and Johnson 2010). For example, water flushes freely through the inductive cell,  
74 significantly lowering power consumption compared to sensors using pumped electrode  
75 conductivity cells. Also, due to the absence of a direct coupling with seawater, inductive cells do

76 not have problems with oil contamination or corrosion, both of which largely degrade the  
77 performance of metal electrodes.

78 Inductive conductivity sensors produced by Falmouth Scientific, Inc. (FSI) were installed on the  
79 first experimental Profiling Autonomous Lagrangian Circulation Explorers (PALACE) floats in  
80 1990s and deployed mostly by the Woods Hole Oceanographic Institution (Bacon et al. 2001;  
81 Durand and Reverdin 2005). However, the performance of FSI CTD-equipped Argo floats was  
82 substandard, and the cells were subsequently phased out (the last FSI-equipped Argo float was  
83 deployed in December 2006) (Abraham et al. 2013). The poor performance of FSI CTDs was  
84 associated with biofouling mitigation techniques (ablative coatings) that changed the cell  
85 geometry and caused conductivity drift. The potential for mitigative measures resulted from the  
86 relatively long presence (sometimes longer than 24 h) of the float at the ocean surface, which  
87 was required for data transmission through the ARGOS satellite system. FSI CTDs also suffered  
88 from issues that are not inherent to inductive conductivity sensors. For example, a firmware fault  
89 in the data bin averaging algorithm resulted in a pressure bias that could not be corrected in post-  
90 processing (Barker et al. 2011). As a result of the problems plaguing the FSI CTD, and perhaps a  
91 lack of interest from competing manufacturers, an overwhelming majority of CTD instruments  
92 installed on Argo profilers use Sea-Bird's electrode-based CTDs.

93 A series of recent setbacks and technological improvements have motivated the development of  
94 a new sensor package for Core Argo floats. The switch to Iridium telemetry has reduced the time  
95 a float spends at the surface from 12–24 hours to 15–20 min. The shorter time spent at the  
96 surface means there is less of a need for biofouling mitigation, a problem that has historically  
97 plagued both electrode-based and inductive cells. Additionally, pump-free CTDs consume much

98 less power, which directly translates into longer float lifetime. Finally, there has been a call to  
99 diversify the sensor packages on Argo floats so that the program is not susceptible to "single  
100 points of failure" (Roemmich et al. 2019).

101 The goal of this study is to assess the long-term accuracy and stability of salinity measurements  
102 collected by four Argo floats equipped with the RBR*argo* inductive CTD manufactured by RBR  
103 Ltd. (<https://rbr-global.com/>). All four floats were deployed in the western Pacific Ocean as  
104 either experimental or pilot-project Argo floats (Figure 1). For this analysis, we use the standard  
105 Argo community OWC MATLAB toolbox ([https://github.com/ArgoDMQC/matlab\\_owc](https://github.com/ArgoDMQC/matlab_owc))  
106 combined with a custom MATLAB visualization toolbox designed to help Argo users to select  
107 appropriate settings for OWC processing and make defensible conclusions about accuracy and  
108 stability of conductivity sensors.

109 The paper is organized as follows: The data and methods of data analysis are described in  
110 Section 2. Section 3 presents the results. First, the stability characteristics calculated by OWC  
111 method for four RBR*argo* floats are analyzed and compared to the initial accuracy assessments.  
112 Second, these statistics are compared to salinity drift and bias estimated during DMQC and  
113 applied to other floats operating in the same regions. Then, the methods helping to avoid  
114 misinterpretation of the results of OWC analysis are demonstrated. Finally, a discussion is  
115 presented in section 4.

## 116 **2. Data and Method**

### 117 ***2.1. Argo floats equipped with inductive conductivity sensors***

118 Four Argo Teledyne Webb Research Autonomous Profiling Explorer (Apex) floats equipped  
119 with RBR*argo* CTDs with inductive conductivity cells were deployed in the western Pacific  
120 Ocean in 2015 and 2018 (Figure 1; Table 1).

121 The RBR*argo* CTD design changed in 2016, meaning the CTD on float 5904925 differs from the  
122 CTD on floats 2903005, 2903327, and 2902730 (Figure 2). The 2016 redesign was undertaken  
123 to improve the dynamic performance of the RBR*argo* CTD. Two modifications were made: 1)  
124 the thermistor was moved onto the conductivity cell itself, thereby eliminating the time lag from  
125 spatial mismatches of the sensors, and 2) the body of the cell was optimized to ensure the  
126 thermistor samples undisturbed water (Argo Steering Team 2018). Both CTD cell designs  
127 measure conductivity with induction.

128 All Argo floats operate on a nominal 10-day cycle. For most of that cycle, they drift at a “parking  
129 depth”, typically 1000 m. Once in each cycle, the float dives to a 2000 m depth by changing its  
130 buoyancy and then performs an upcast profile measuring the Core Argo variables (pressure,  
131 temperature, and conductivity) up to the ocean surface. At the surface, the information is  
132 transmitted via satellite and the float descends back to its parking depth. The battery capacity of  
133 the float allows for at least 150 CTD profiles, which gives the float a theoretical four-year  
134 lifespan assuming a 10-day cycle.

135 Argo data telemetered via satellite are transmitted to one of the 11 Argo regional Data Assembly  
136 Centers (DAC) where they are checked for outliers by coarse semi-automatic RTQC tests (Wong  
137 et al. 2020). This data product, referred to as NRT, is then sent to Argo Global Data Assembly  
138 Centers (GDACs) and made publicly available within 24 h. DMQC analysis is then performed  
139 by DACs to produce a delayed-mode data product, available within 12 months after observation.

140 During the DMQC analysis, salinity observations are carefully checked by experts and, if  
141 necessary, corrected using the OWC method, a standard method for the Argo community (Wong  
142 et al. 2020).

## 143 ***2.2. Salinity bias and drift detection***

144 The OWC analysis is the statistical method of salinity drift correction described in Owens and  
145 Wong (2009) and Cabanes et al. (2016). In this method, the salinity profiles observed by an Argo  
146 float are compared to reference data in the same region by using objective mapping (OM;  
147 Bretherton et al. 1976). In this study, we used separately two reference datasets approved and  
148 used by the Argo community and prepared by the Argo Data Management Team (ADMT) at the  
149 Coriolis Data Centre: 1) shipboard CTD casts (CTD\_for\_DMQC) and 2) DMQC-corrected Argo  
150 profiles collected during preceding years (Argo\_for\_DMQC). Both datasets are available for the  
151 members of the Argo program upon request to the *Institut Français de Recherche pour*  
152 *l'Exploitation de la Mer* (IFREMER).

153 Based on the fact that water-mass structures can be defined by the relations between potential  
154 temperature and salinity, the salinity measured by Argo float is compared to the reference along  
155 as many as 10 potential temperature isotherms, characterized by minimal salinity variations and  
156 ‘calibrated’ by the weighted least squares method to minimize its difference from the reference.  
157 The weights for the calculation are proportional to the inverse of the OM errors such that less  
158 variable deep-layer climatology influences the ‘calibration’ of float salinity more than those of  
159 the more variable surface and intermediate layers.

160 In the OM calculations, the selection of reference data for each profile and their respective  
161 weights depend on their distance from the observed profiles in space and time: highest weights  
162 are assigned to reference profiles most closely positioned and most contemporaneous to the float  
163 profile date, as well as those with measurements obtained on the same isobaths as the float  
164 profile (Böhme and Send 2005). OM is performed in two steps, by first fitting large-scale  
165 variability and then small-scale residuals. The parameters regulating these scales are referred to  
166 as decorrelation scales and are selected by the user on the basis of his/her knowledge of the  
167 effect of these factors on the objective mapping in the study region (Wong et al. 2003). The  
168 OWC method is based on the assumption that any conductivity offset changes slowly over time;  
169 as a result, a piecewise linear fit of the profile-based corrections over the float time series is  
170 applied. The OWC analysis returns a set of salinity correction factors, one for each completed  
171 profile. The decision whether or not the statistical trends represent sensor drift or ocean  
172 variability, and in turn whether or not conductivity corrections should be applied, is made by the  
173 user and involves some subjectivity.

174 The OWC MATLAB toolbox settings used in this study are listed in the Appendix.

### 175 ***2.3. Distinguishing between instrumental errors and oceanographic variability***

176 The results of the OWC output strongly depend on the quality of reference data. Anomalies in  
177 salinity measured by the float CTD relative to water mass with different temperature-salinity  
178 characteristics can be easily misinterpreted as sensor drift, especially when reference data are  
179 sparse or inaccurate. The approach taken in this study relies on visualization methods designed to  
180 assist users to determine whether anomalies in measured salinity are caused by instrumental

181 errors or oceanographic variability and, as such, avoid ambiguity in salinity drift detection. These  
182 methods include:

- 183 1. Plots showing 1) a time series of the profile fit coefficients (calculated by the OWC  
184 method as the vertically averaged reference salinities minus corrected float salinities at 10  
185 selected reference potential temperature levels) and 2) a map showing the magnitude of  
186 the fit coefficients along the float trajectory. Such plots help to identify spatial coherency  
187 in discrepancies between the analyzed Argo measurements and the reference dataset,  
188 providing information on whether discrepancies should be attributed to errors in the  
189 reference data, or to sensor drift.
- 190 2. Diagrams comparing the objectively mapped reference salinity field calculated by the  
191 OWC method to a different reference data source. For this purpose, the nearest grid  
192 points of the World Ocean Atlas (2005-2017) monthly climatology of 1° resolution  
193 (WOA1) (Garcia et al. 2018) and/or other monthly gridded datasets were used.  
194 Discrepancies between different reference sources support the hypothesis that large  
195 salinity anomalies might be due to inappropriate reference data, rather than to sensor  
196 drift.
- 197 3. Simplified OWC analysis of nearby contemporary Argo floats provides yet another  
198 indication of whether the computed salinity error emanates from the reference dataset  
199 used.

## 200 **3. Results**

### 201 *3.1. Salinity offsets and their dependence on reference data and time separation factors*

202 The OWC analysis, when run with the settings specified in the Appendix against the two  
203 ADMT-CTD and ADMT-Argo reference databases, revealed no statistical trends in any of the  
204 four RBR*argo* float salinities. There were small differences between the salinities measured by  
205 the RBR*argo* and the reference data. When compared to the ADMT-Argo reference database, the  
206 salinity offsets were much smaller than the offsets based on the ADMT-CTD reference database  
207 (Table 2). We speculate that these differences result from different time periods when the  
208 reference data were collected (Figure 3). Most CTD casts were collected during 1980s-1990s  
209 (Figure 3-b3, c3); only in the Northwest Pacific a large number of CTD casts was taken after  
210 2000 (Figure 3-a3). In contrast, most Argo profiles were collected after 2005 (Figure 3-a4, b4,  
211 c4). Comparing these data to RBR*argo* floats operating during the recent 2–4 years resulted in  
212 disagreement associated with long-term salinity variations in the Pacific Ocean documented in  
213 previous studies (e.g. Boyer et al. 2005; Durack and Wijffels 2010; Helm et al. 2010).

214 The salinity offset for Argo Australia float 5904925 in the Coral Sea demonstrated significant  
215 salinity bias: -0.0100 to -0.0132 when compared to ADMT-Argo reference data collected during  
216 the recent 15 years and -0.0152 to -0.0167 when compared to ADMT-CTD data collected mostly  
217 20–35 years ago (Table 2). This offset exceeds the Argo accuracy limits (0.01) and may result  
218 from the fact that this float was equipped with old-design C-cell, although the conclusion about  
219 better accuracy of CT-cells have to be confirmed by additional data.

220 For three RBR*argo* floats equipped with CT-cells of new design (two Japan Argo floats in the  
221 Northwest Pacific and the China Argo float in the Philippine Sea), OWC comparison to ADMT-  
222 Argo reference dataset with a relatively small (1–3 years) time separation factor resulted in  
223 salinity offsets between -0.0009 and -0.0020, well below the Argo accuracy limits (Table 2).

224 Larger time separation factors resulted in larger offsets, especially for both Japan Argo floats.  
225 We attribute this fact to recent salinity changes in that area. When compared to ADMT-CTD  
226 data, the largest disagreement ( $>0.01$ ) was observed with small (1–3 years) time separation  
227 factors. Small time separation factors mean that *RBRargo* measurements are compared with  
228 most recent measurements, but for the ADMT-CTD database this is a comparatively short time  
229 period 10-15 years ago when the majority of recent ADMT-CTD data was collected (Figure 3-  
230 a3, b3, c3). We may suggest that during that short period salinity was different from the recent  
231 period when the analyzed *RBRargo* data were collected. When the short-scale and large-scale  
232 time separation factors were set to 10 and 30 years, respectively, the resulting offsets decreased  
233 below the Argo accuracy limits (Table 2).

234 The dependence of the OWC results on other settings (see Appendix) was small. Based on these  
235 results, we chose the ADMT-Argo 2019v01 database as a source of reference data and the  
236 following time separation factor values (small/large): 3/10 years for Argo Australia 5904925 and  
237 China Argo 2902730, and 1/3 years for Japan Argo floats 2903005 and 2903317 (Table 2). The  
238 resulting OWC output showed no significant statistical trends for all four floats, which we  
239 interpret to mean that salinity, as measured by the *RBRargo* CTD, does not drift. We concluded  
240 that only salinity measured by one float (Argo Australia 5904925) required a correction in the  
241 form of a constant offset of -0.01; the other three floats did not need a salinity correction  
242 whatsoever.

### 243 **3.2. Initial accuracy of floats**

244 The assessments of the initial accuracies of *RBRargo* salinity measurements indicated that they  
245 were close to the salinity offsets calculated by the OWC method. Assessments were made by

246 comparing the salinity measured in the first few cycles to CTD casts collected shortly after the  
247 float deployments (Figure 4). The differences in salinity along isopycnals (potential density  
248 levels) were computed and averaged over the range of potential temperature below 5°C (Table  
249 3). Only the Argo Australia float deployed in the Coral Sea demonstrated salinity bias exceeding  
250 the Argo accuracy limits ( $>0.01$ ). For the three other floats, the initial accuracy was within the  
251 Argo requirements (Table 3). Comparing the first Argo profiles to the WOA1 climatology  
252 demonstrated larger differences than when compared to the CTD casts. In the Northwest Pacific  
253 and the Philippine Sea, the salinity measured by Argo floats varied mostly within the WOA1  
254 climatology standard deviation limits (Figure 4b, c). In contrast, salinity in the Coral Sea  
255 measured by the starting profile of the Argo float 5904925 exceeded both the CTD and WOA1  
256 salinity variation limits within the entire deep ( $\theta < 5^\circ\text{C}$ ) layer (Figure 4a).

### 257 ***3.3. RBRargo in situ drift and bias correction comparison to the electrode-based CTDs***

258 To put the RBRargo salinity drift analysis in context, we assessed the long-term stability of other  
259 Argo floats equipped with electrode-based SBE41/41CP. To compare the CTDs directly, Argo  
260 datafiles were downloaded from a GDAC for all floats that (1) operated starting 2011 in the same  
261 areas (the  $20^\circ \times 20^\circ$  rectangles around the float trajectories in Figure 1a) and (2) contained a  
262 sufficient number of DM data (at least 25 profiles). A total of 360 floats met these criteria; the  
263 median time of operation was about 4 years, and the median number of DM profiles was 175  
264 (minimum 27 profiles, maximum 438 profiles). For each float, the salinity offsets used for DM  
265 correction were computed from the mean difference between the raw salinity (PSAL) and the  
266 adjusted salinity (PSAL\_ADJUSTED) in all DM profiles. In about 16% of the Argo floats with

267 electrode conductivity sensors (57/360), the applied salinity offsets exceeded 0.01. For 31% of  
268 floats (111/360), the salinity drift exceeded  $0.0025 \text{ yr}^{-1}$ .

269 Only one float with an RBR<sub>argo</sub> CTD (Argo Australia float 5904925) demonstrated a significant  
270 offset (-0.010) relative to ADMT-Argo reference salinity (Figure 5a), which is also the first float  
271 with RBR-equipped conductivity cell deployed in 2015. Since then, the design of the RBR  
272 conductivity cell was improved, with the thermistor located next to the conductivity cell (see  
273 Figure 2b). The three RBR<sub>argo</sub> CTDs with new conductivity cell design (i.e., floats 2902730,  
274 2903005, and 2903327) did not need salinity correction. Their calibration offsets were  
275 significantly lower than the calibration accuracy of ocean salinity measurements claimed by  
276 RBR ( $\sim \pm 0.003$ , or  $\pm 0.003 \text{ mS/cm}$  at  $15^\circ\text{C}$ ) (Halverson et al. 2020). All four RBR<sub>argo</sub> CTDs  
277 demonstrated no salinity drift, although in many floats equipped with electrode conductivity cells  
278 salinity drift was detected and corrected during the DMQC analysis (Figure 5b).

### 279 ***3.4. Detecting problematic reference data in salinity drift assessment***

280 The OWC calibration method, when applied to data from four RBR<sub>argo</sub>, indicated that the CTDs  
281 are very stable over a two or more years. However, there remain anomalies in the calibration  
282 salinity that warrant further investigation because, as a statistical method, OWC cannot  
283 determine whether variations in the calibration salinity are related to sensor problems or  
284 oceanographic variability. In this section, we describe in detail the results from the OWC output  
285 of four RBR<sub>argo</sub> floats and demonstrate the methods helping us to avoid this kind of ambiguity.  
286 The approach we use includes (1) identifying spatial coherency in discrepancies between the  
287 analyzed Argo measurements and the reference dataset, (2) comparing the reference salinity

288 fields calculated by the OWC to a different reference data source, and (3) applying the OWC  
289 analysis to other nearby contemporary Argo floats.

#### 290 *3.4.1. Argo Australia float 5904925 in the Coral Sea*

291 For the Argo Australia float 5904925 deployed in the Coral Sea, the computed fit coefficients  
292 were comparable in the beginning (July 2015–April 2016) and the end (March 2018–August  
293 2019) of the dataset, demonstrating a high level of the sensor stability (Figure 6a). The computed  
294 salinity offset, however, was significantly different in-between those two time periods. A more  
295 detailed analysis demonstrated that the deviations from the average offset were spatially  
296 coherent, suggesting that the discrepancy might be due a specific oceanographic feature that was  
297 measured by the float, but not captured by the reference dataset. In fact, for Argo Australia float  
298 5904925, the geographical location of these deviations clearly demonstrates that all profiles with  
299 salinity offsets anomalously larger than -0.010 were concentrated in the area to the south-  
300 southeast from the Solomon Islands, between 11°S–13°S and 161°E–165°E (Figure 6b).  
301 Additional evidence of shortcomings of the reference dataset arises from the comparison  
302 between the reference salinity calculated by the OWC OM algorithm on the basis of the ADMT-  
303 Argo dataset to the World Ocean Atlas 1° resolution 2005-2017 climatology (WOA1, Figure 6c).  
304 A large discrepancy is observed during the same time period when the reference Argo dataset  
305 yielded larger salinity. Comparison between the ADMT-Argo reference data and other  
306 climatologies and gridded monthly products (World Ocean Atlas 1955-2017 of 0.25° resolution  
307 WOA4 (Garcia et al. 2018); Monthly Isopycnal & Mixed-layer Ocean Climatology MIMOC  
308 (Schmidt et al. 2013); CSIRO Atlas of Regional Seas CARS2009 (Ridgway et al.  
309 2002); Roemmich-Gilson Argo Climatology RG (Roemmich and Gilson 2009)) demonstrated

310 similar results. We concluded that the variations in the salinity profile fit coefficients calculated  
311 by the OWC method from the ADMT-Argo reference dataset was likely be attributed to  
312 shortcomings in the reference data rather than to sensor drift.

#### 313 *3.4.2. Japan Argo floats 2903005 and 2903327 in the Northwest Pacific*

314 The OWC output for of the two Japan Argo floats in the Northwest Pacific did not show a  
315 statistically significant trend in salinity, and it returned salinity offsets well below salinity  
316 measurement accuracy (+0.0009 for float 2903005 and +0.0017 for float 2903327; see Table 2  
317 and Figures 7a and 8a). These results, however, strongly depend on the time separation factors  
318 (see Table 2). The salinity offsets closest to zero were obtained when the small/large factors were  
319 set to 1/3 years, the values recommended for highly variable regions like the North Atlantic  
320 (Cabanès et al. 2016).

321 Although the OWC output did not show a statistical trend in both Japan Argo floats, the  
322 differences between the salinity measured by the float 2903005 and reference salinity  
323 demonstrated substantial changes over time: a maximum in September 2018 followed by a  
324 gradual decrease until May 2019 (Figure 7a). Spatial analysis of these variations once again  
325 shows spatial coherency (Figure 7b). Comparing the OWC OM output to the WOA1 climatology  
326 demonstrates that the variations in the profile fit coefficients are correlated with the differences  
327 between the reference data and WOA1 (Figure 7c). Profile fit coefficients were positive between  
328 February 2018 and November 2018, and negative over the period ranging from February 2019  
329 and September 2019. During the first half of the times series, float 2903005 was located in the  
330 water with salinity significantly higher than captured by WOA1, which may be explained by  
331 recent changed in salinity in the Pacific Ocean (Figure 5c) (Li et al. 2019; Liu et al. 2019; Wang

332 et al. 2017). During the latter half of the time series, the float moved to the northwest before  
333 being advected by strong currents and transported to west-southwest, covering about 240 km in  
334 less than a month (March 16, 2019–April 12, 2019), resulting in a mean trajectory velocity  
335 greater than  $10 \text{ cm s}^{-1}$ . This relocation of the float to a different region affected by the Kuroshio  
336 extension was associated with water characterized by lower salinity, which is evident from the  
337 large positive anomaly observed between the reference dataset and WOA1 (Figure 7c) before  
338 relocation and no significant difference after. Once again, these results are independent of the  
339 climatology considered.

340 The salinity measured by the Japan Argo float 2903327 was on the average within 0.0017 of the  
341 salinity in the reference dataset (Figure 8a). As with float 2903005, the comparison between the  
342 reference salinity in the ADMT-Argo dataset and the WOA1 climatology demonstrated strong  
343 disagreement (Figure 8c), except during the first few months, when the float was located to the  
344 south of  $30^\circ\text{N}$  (Figure 8b). Float 2903327 also moved to the region where float 2903005 was  
345 taken by strong current and transported to water with different temperature-salinity properties  
346 ( $32^\circ\text{N}$ ;  $160^\circ\text{E}$ ). However, it arrived to that region about two months later, which might explain  
347 why the salinity variations observed in the data collected by float 2903005 were not observed by  
348 float 2903327.

#### 349 *3.4.3. China Argo float 2902730 in the Philippine Sea*

350 The results of OWC analysis of the China Argo float 2902730 in the Philippine Sea demonstrate  
351 close correspondence between the measured and reference salinity, except during the last 4  
352 months of the time series, when the profile fit coefficients are negative and reach -0.0112 (Figure  
353 9a). During that period, the float drifted to the north of  $14^\circ\text{N}$  and remained in this region until the

354 end of the time series (green rectangle in Figure 9b). Comparison between the reference data and  
355 all five climatologies did not reveal significant disagreement during that period, in contrast to  
356 other floats analyzed in this study (Figure 9c). Instead, the negative offset observed after July  
357 2019 is attributed to a large decrease in the number of simultaneously collected reference data, as  
358 DM Argo data would only be available minimum 6 months after collection. To confirm this  
359 hypothesis, this trend observed in OWC results is further analyzed.

360 To verify that the disagreement in salinity in this area was not related to sensor drift, we  
361 extracted from the GDAC all data from floats profiling in the same area (14°N–17°N; 126°E–  
362 129°E; green rectangles in Figures 9b and 10b) during the same period (starting July 2019),  
363 which is comprised of NRT data exclusively. Six floats with more than 10 profiles were selected  
364 for comparison (2902703, 2902708, 2902688, 2902683, 2902707 and 2901545). All six floats  
365 demonstrated similar decrease of the OWC profile fit coefficients in that small area. Results for  
366 float 2902683 are shown in Figure 10; other floats are not shown for clarity. It is interesting that  
367 the large negative  $\Delta S$  starting January 2019 is not seen in the OWC vs WOA1 comparison  
368 (Figure 10c); we attribute this fact to recent salinity changes in the Pacific Ocean (Li et al. 2019;  
369 Liu et al. 2019; Wang et al. 2017).

#### 370 **4. Discussion**

371 This study demonstrates the high level of accuracy and stability of salinity data collected by the  
372 RBR*argo* CTDs. When analyzed by the standard OWC method with default settings, all four  
373 RBR*argo* floats operating in the Pacific Ocean revealed no drift and only one of them deployed  
374 more than four years ago and equipped with C-cell of old design demonstrated a calibration  
375 offset of -0.010, right at the limit of Argo guidelines. All three RBR*argo* equipped with CT-cells

376 of new design collected data which do not require correction. These characteristics look  
377 promising, taking into account that many Argo floats with electrode conductivity sensors  
378 produce measurements that require a salinity offset and/or drift correction. Of 360 Argo floats  
379 operating in the same areas, >30% demonstrated significant drift (>0.01 in 4 years) corrected  
380 during DMQC processing. Statistics for previous years reveal similar figures: for example, about  
381 75% of Argo profiles in the COriolis dataset for Re-Analysis (CORA3) (1999-2010), had to be  
382 adjusted for pressure and/or salinity offset (Cabanès et al. 2013).

383 The OWC analysis of salinity stability of data collected by Argo floats demonstrated some  
384 caveats, which can result in subjectivity in the application of a salinity drift correction. These  
385 caveats are associated with limitations of reference data, which can naively be misinterpreted as  
386 sensor drift. The likelihood of a float encountering salinities different from the reference data is  
387 expected to be higher in the areas characterized by high gradients and increased variability of  
388 salinity in deep layers selected by the OWC analysis. This is illustrated by the patterns of  
389 geographical distribution of WOA1 salinity mean and standard deviation averaged over the  
390 1000–1200 dbar layer (Figure 11). In the Coral Sea, the most problematic area (in terms of  
391 reference salinity) was the region between the Solomon Islands and Vanuatu (Figures 6b, 11a,  
392 d). The intermediate waters (>700 dbar) in that area are dominated by the low-salinity Antarctic  
393 Intermediate Water (AAIW) transported from the south (Gasparin et al. 2014; Qu and Lindstrom  
394 2004). The northern extension of the AAIW terminates in a strong salinity front (Sokolov and  
395 Rintoul 2000) (Figure 11a). We speculate that during the objective mapping, high salinity  
396 measured to the north from this sharp gradient added positive bias to the reference data to the  
397 south resulting in the observed disagreement (Figure 6b).

398 The disagreement between the salinity measured by the Japan Argo float and the reference data  
399 (Figure 7a, b) increased when the float drifted northwest to the area affected by the Kuroshio  
400 extension characterized by high salinity variations (Qiu 2001) (Figure 11e). A similar pattern  
401 was observed in the Philippine Sea where the China Argo float was drifting northward to the area  
402 where the main part of the Pacific North Equatorial Current bifurcates and feeds the northward  
403 flowing Kuroshio and the southward flowing Mindanao Current (Qiu and Lukas 1996; Wang et  
404 al. 2015). Salinity in the northern part of the Philippine Sea is lower and more variable as  
405 compared to the area to the south (Figure 11c, f) (Zhou et al. 2018), and the northward trajectory  
406 of the Argo float resulted in gradual increase of the disagreement between the measurements and  
407 the references (Figure 9a, b).

408 The importance of reference data for salinity drift assessment was evident from the beginning of  
409 the Argo program (Gaillard et al. 2009; Kobayashi and Minato 2005). Previous studies  
410 demonstrated an increase in the number of Argo profiles erroneously attributed as suspicious in  
411 dynamic and weakly stratified regions like the North Atlantic (Böhme and Send 2005; Cabanes  
412 et al. 2016), high eddy kinetic energy regions such as Western Boundary Currents (Jia et al.  
413 2016; Wang et al. 2013), or during anomalous events such as the El Niño–Southern Oscillation  
414 (ENSO) (Cabanes et al. 2013). This study also demonstrates the importance of long-term trends  
415 in salinity which must be taken into account in OWC analysis. We see that increasing the OWC  
416 time separation factor causes the Argo DMQC reference databases to approach climatology,  
417 while current conditions are different from climatological values. Although a sufficient number  
418 of high-quality reference data and proper selection of parameter settings for OWC  
419 calculations are a primary requirement for proper assessment of Argo sensor stability,  
420 visualization approaches like the ones demonstrated here can provide significant help. We

421 recommend these methods for Argo users and believe that they can help Argo community in its  
422 mission – collecting high-quality oceanographic observations.

### 423 **Data Availability Statement**

424 The Argo data is freely available from the Argo program website  
425 ([http://www.argo.ucsd.edu/Argo\\_data\\_and.html](http://www.argo.ucsd.edu/Argo_data_and.html)).

### 426 **Acknowledgments**

427 The data from the Argo Australia, China Argo and Japan Argo floats used here were collected  
428 and are made freely available by the International Argo program and the national programs that  
429 contribute to it. G. Maze was supported by the EARISE project, a European Union’s Horizon  
430 2020 research and innovation program under grant agreement no 824131, call INFRADEV-03-  
431 2018-2019: Individual support to ESFRI and other world-class research infrastructures. We  
432 acknowledge Susan Wijffels, who provided advice on reference climatologies, coordinated  
433 access to the data from Argo Australia float 5904925, and provided ship CTD data to evaluate  
434 the initial accuracy of the float. Toshio Suga and Shigeki Hosoda provided ship CTD data for  
435 assessing the initial accuracy of Japan Argo floats 2903005 and 2903327. We would like to  
436 thank Zenghong Liu for coordinating access to ship CTD data and continued discussion  
437 regarding RBR*argo* CTD accuracy and stability. We thank Annie P. S. Wong for critical  
438 comments and recommendations in data analysis. We thank Mathieu Dever for critical reading  
439 and comments for the manuscript. Finally, we wish to thank the Argo Steering Team for  
440 encouraging Argo member nations to take part in the RBR CTD Argo Global Pilot Project.

### 441 **Appendix**

442 The OM interpolation of reference data by OWC MATLAB toolbox was performed with the  
443 settings listed in Table A1. The parameters regulating linear fit of the profile-based corrections  
444 were set to default values, i.e., the number of breakpoints was selected automatically.

445

446 **References**

- 447 Abraham, J. P., and Coauthors, 2013: A review of global ocean temperature observations:  
448 Implications for ocean heat content estimates and climate change. *Reviews of Geophysics*,  
449 **51**(3), 450–483, <https://doi.org/10.1002/rog.20022>.
- 450 Argo Steering Team, 2018: 19th meeting of the International Argo Steering Team, Sidney, B.C.,  
451 Canada, March 12-15, 2018, 1-159 pp.
- 452 Bacon, S., L. R. Centurioni, and W. J. Gould, 2001: The evaluation of salinity measurements  
453 from PALACE floats. *Journal of Atmospheric and Oceanic Technology*, **18**(7), 1258-  
454 1266, [https://doi.org/10.1175/1520-0426\(2001\)018<1258:TEOSMF>2.0.CO;2](https://doi.org/10.1175/1520-0426(2001)018<1258:TEOSMF>2.0.CO;2).
- 455 Barker, P. M., J. R. Dunn, C. M. Domingues, and S. E. Wijffels, 2011: Pressure sensor drifts in  
456 Argo and their impacts. *Journal of Atmospheric and Oceanic Technology*, **28**(8), 1036-  
457 1049, <https://doi.org/10.1175/2011JTECHO831.1>.
- 458 Böhme, L., and U. Send, 2005: Objective analyses of hydrographic data for referencing profiling  
459 float salinities in highly variable environments. *Deep-Sea Research II*, **52**(3-4), 651–664,  
460 <https://doi.org/10.1016/j.dsr2.2004.12.014>.
- 461 Boyer, T. P., S. Levitus, J. I. Antonov, R. A. Locarnini, and H. E. Garcia, 2005: Linear trends in  
462 salinity for the World Ocean, 1955–1998. *Geophysical Research Letters*, **32**(1),  
463 <https://doi.org/10.1029/2004gl021791>.
- 464 Bretherton, F., R. Davis, and C. Fandry, 1976: A technique for objective analysis and design of  
465 oceanic experiments applied to Mode-73. *Deep-Sea Research II*, **23**(7), 559–582,  
466 [https://doi.org/10.1016/0011-7471\(76\)90001-2](https://doi.org/10.1016/0011-7471(76)90001-2).
- 467 Cabanes, C., V. Thierry, and C. Lagadec, 2016: Improvement of bias detection in Argo float  
468 conductivity sensors and its application in the North Atlantic. *Deep-Sea Research I*, **114**,  
469 128-136, <https://doi.org/10.1016/j.dsr.2016.05.007>.
- 470 Cabanes, C., and Coauthors, 2013: The CORA dataset: validation and diagnostics of in-situ  
471 ocean temperature and salinity measurements. *Ocean Science*, **9**, 1–18,  
472 <https://doi.org/10.5194/os-9-1-2013>.
- 473 Durack, P. J., and S. E. Wijffels, 2010: Fifty-Year Trends in Global Ocean Salinities and Their  
474 Relationship to Broad-Scale Warming. *Journal of Climate*, **23**(16), 4342-4362,  
475 <https://doi.org/10.1175/2010jcli3377.1>.
- 476 Durand, F., and G. Reverdin, 2005: A statistical method for correcting salinity observations from  
477 autonomous profiling floats: An ARGO perspective. *Journal of Atmospheric and*  
478 *Oceanic Technology*, **22**(3), 292-301, <https://doi.org/10.1175/JTECH1693.1>.

- 479 Fofonoff, N. P., 1985: Physical properties of seawater: A new salinity scale and equation of state  
480 for seawater. *Journal of Geophysical Research: Oceans*, **90**(C2), 3332-3342,  
481 <https://doi.org/10.1029/JC090iC02p03332>.
- 482 Gaillard, F., E. Autret, V. Thierry, P. Galaup, C. Coatanoan, and T. Loubrieu, 2009: Quality  
483 control of large Argo datasets. *Journal of Atmospheric and Oceanic Technology*, **26**(2),  
484 337-351, <https://doi.org/10.1175/2008jtecho552.1>.
- 485 Garcia, H. E., and Coauthors, 2018: World Ocean Atlas 2018 (pre-release): Product  
486 Documentation.
- 487 Gasparin, F., C. Maes, J. Sudre, V. Garcon, and A. Ganachaud, 2014: Water mass analysis of the  
488 Coral Sea through an Optimum Multiparameter method. *Journal of Geophysical  
489 Research: Oceans*, **119**(10), 7229-7244, <https://doi.org/10.1002/2014jc010246>.
- 490 Halverson, M., E. Siegel, and G. Johnson, 2020: Inductive-conductivity cell. *Sea Technology*,  
491 **61**(2), 24-27.
- 492 Helm, K. P., N. L. Bindoff, and J. A. Church, 2010: Changes in the global hydrological-cycle  
493 inferred from ocean salinity. *Geophysical Research Letters*, **37**(18),  
494 <https://doi.org/10.1029/2010gl044222>.
- 495 Jayne, S. R., D. Roemmich, N. Zilberman, S. C. Riser, K. S. Johnson, G. C. Johnson, and S. R.  
496 Piotrowicz, 2017: The Argo program: Present and future. *Oceanography*, **30**(2), 18-28.
- 497 Jia, W., D. Wang, N. Pinardi, S. Simoncelli, A. Storto, and S. Masina, 2016: A quality control  
498 procedure for climatological studies using Argo data in the North Pacific Western  
499 Boundary Current region. *Journal of Atmospheric and Oceanic Technology*, **33**(12),  
500 2717-2733, <https://doi.org/10.1175/JTECH-D-15-0140.1>.
- 501 Kobayashi, T., and S. Minato, 2005: Importance of reference dataset improvements for Argo  
502 Delayed-Mode Quality Control. *Journal of Oceanography*, **61**(6), 995-1009,  
503 <https://doi.org/10.1007/s10872-006-0016-z>.
- 504 Legler, D. M., and Coauthors, 2015: The current status of the real-time in situ Global Ocean  
505 Observing System for operational oceanography. *Journal of Operational Oceanography*,  
506 **8**, s189-s200, <https://doi.org/10.1080/1755876X.2015.1049883>.
- 507 Li, G., Y. Zhang, J. Xiao, X. Song, J. Abraham, L. Cheng, and J. Zhu, 2019: Examining the  
508 salinity change in the upper Pacific Ocean during the Argo period. *Climate Dynamics*,  
509 **53**(9-10), 6055-6074, <https://doi.org/10.1007/s00382-019-04912-z>.
- 510 Liu, C., X. Liang, R. M. Ponte, N. Vinogradova, and O. Wang, 2019: Vertical redistribution of  
511 salt and layered changes in global ocean salinity. *Nature Communications*, **10**(1), 3445,  
512 <https://doi.org/10.1038/s41467-019-11436-x>.
- 513 McDougall, T. J., and P. M. Barker, 2011: *Getting started with TEOS-10 and the Gibbs Seawater*  
514 *(GSW) Oceanographic Toolbox*. SCOR/IAPSO WG127, 28 pp.

- 515 Owens, W. B., and A. P. S. Wong, 2009: An improved calibration method for the drift of the  
516 conductivity sensor on autonomous CTD profiling floats by  $\theta$ -S climatology. *Deep-Sea*  
517 *Research I*, **56**(3), 450-457, <https://doi.org/10.1016/j.dsr.2008.09.008>.
- 518 Qiu, B., 2001: Kuroshio and Oyashio Currents. *Encyclopedia of Ocean Sciences*, J. H. Steele, S.  
519 A. Thorpe, and K. K. Turekian, Eds., Academic Press, 1413-1425.
- 520 Qiu, B., and R. Lukas, 1996: Seasonal and interannual variability of the North Equatorial  
521 Current, the Mindanao Current, and the Kuroshio along the Pacific western boundary.  
522 *Journal of Geophysical Research: Oceans*, **101**(C5), 12315-12330,  
523 <https://doi.org/10.1029/95JC03204>.
- 524 Qu, T., and E. J. Lindstrom, 2004: Northward Intrusion of Antarctic Intermediate Water in the  
525 Western Pacific. *Journal of Physical Oceanography*, **34**(9), 2104-2118,  
526 [https://doi.org/10.1175/1520-0485\(2004\)034<2104:NIOAIW>2.0.CO;2](https://doi.org/10.1175/1520-0485(2004)034<2104:NIOAIW>2.0.CO;2).
- 527 Ridgway, K. R., J. R. Dunn, and J. L. Wilkin, 2002: Ocean interpolation by four-dimensional  
528 least squares - Application to the waters around Australia. *Journal of Atmospheric and*  
529 *Oceanic Technology*, **19**(9), 1357-1375, [https://doi.org/10.1175/1520-0426\(2002\)019<1357:OIBFDW>2.0.CO;2](https://doi.org/10.1175/1520-0426(2002)019<1357:OIBFDW>2.0.CO;2).
- 531 Riser, S. C., and Coauthors, 2016: Fifteen years of ocean observations with the global Argo  
532 array. *Nature Climate Change*, **6**(2), 145-153, <https://doi.org/10.1038/nclimate2872>.
- 533 Roemmich, D., and J. Gilson, 2009: The 2004-2008 mean and annual cycle of temperature,  
534 salinity, and steric height in the global ocean from the Argo Program. *Progress in*  
535 *Oceanography*, **82**(2Oceanography), 81-100,  
536 <https://doi.org/10.1016/j.pocean.2009.03.004>.
- 537 Roemmich, D., and Coauthors, 2019: On the future of Argo: A global, full-depth, multi-  
538 disciplinary array. *Frontiers in Marine Science*, **6**(439), 1-28,  
539 <https://doi.org/10.3389/fmars.2019.00439>.
- 540 Schmidtko, S., G. C. Johnson, and J. M. Lyman, 2013: MIMOC: A global monthly isopycnal  
541 upper-ocean climatology with mixed layers. *Journal of Geophysical Research: Oceans*,  
542 **118**(4), 1658-1672, <https://doi.org/10.1002/jgrc.20122>.
- 543 Shkvorets, I., and F. Johnson, 2010: Advantages in performance of the RBR conductivity  
544 channel with Delrin<sup>TM</sup>/ceramic inductive cell. *OCEANS 2010 MTS/IEEE, 20-23 Sept.*  
545 *2010*, Seattle, WA, USA, 1-8.
- 546 Sokolov, S., and S. Rintoul, 2000: Circulation and water masses of the southwest Pacific: WOCE  
547 Section P11, Papua New Guinea to Tasmania. *Journal of Marine Research*, **58**(2), 223-  
548 268, <https://doi.org/10.1357/002224000321511151>.
- 549 Udaya Bhaskar, T. V. S., R. V. Shesu, E. P. R. Rao, and R. Devender, 2013: GUI based  
550 interactive system for Visual Quality Control of Argo data. *Indian Journal of Geo-*  
551 *Marine Sciences*, **42**, 580-586.

- 552 Wang, F., N. Zang, Y. Li, and D. Hu, 2015: On the subsurface countercurrents in the Philippine  
553 Sea. *Journal of Geophysical Research: Oceans*, **120**(1), 131-144,  
554 <https://doi.org/10.1002/2013jc009690>.
- 555 Wang, G., L. Cheng, T. P. Boyer, and C. Li, 2017: Halosteric Sea Level Changes during the  
556 Argo Era. *Water*, **9**(7), 484, <https://doi.org/10.3390/w9070484>.
- 557 Wang, X., G. Han, W. Li, X. Wu, and X. Zhang, 2013: Salinity drift of global Argo profiles and  
558 recent halosteric sea level variation. *Global and Planetary Change*, **108**, 42-55,  
559 <https://doi.org/10.1016/j.gloplacha.2013.06.005>.
- 560 Wedd, R., M. Stringer, and K. Haines, 2015: Argo real-time quality control intercomparison.  
561 *Journal of Operational Oceanography*, **8**(2), 108-122,  
562 <https://doi.org/10.1080/1755876X.2015.1087186>.
- 563 Wong, A. P. S., G. C. Johnson, and W. B. Owens, 2003: Delayed-mode calibration of  
564 autonomous CTD profiling float salinity data by  $\theta$ -S climatology. *Journal of*  
565 *Atmospheric and Oceanic Technology*, **20**(2), 308-318, [https://doi.org/10.1175/1520-0426\(2003\)020<0308:DMCOAC>2.0.CO;2](https://doi.org/10.1175/1520-0426(2003)020<0308:DMCOAC>2.0.CO;2).
- 567 Wong, A. P. S., R. Keeley, T. Carval, and Argo Data Management Team, 2020: Argo Quality  
568 Control Manual for CTD and Trajectory Data.
- 569 Zhou, C., W. Zhao, J. Tian, Q. Yang, X. Huang, Z. Zhang, and T. Qu, 2018: Observations of  
570 Deep Current at the Western Boundary of the Northern Philippine Basin. *Scientific*  
571 *Reports*, **8**(1), 14334, <https://doi.org/10.1038/s41598-018-32541-9>.  
572

573 **Tables**

574

575 Table 1. Four Argo floats with RBR*argo* CTDs operating in the Pacific Ocean.

| <b>Float<br/>WMOID</b> | <b>Region</b>        | <b>Deployment<br/>date</b> | <b>Deployment<br/>coordinates</b> | <b>Vessel</b>            | <b>Operator</b>   | <b>No of<br/>cycles<br/>analyzed</b> |
|------------------------|----------------------|----------------------------|-----------------------------------|--------------------------|---|--------------------------------------|
| 5904925                | Coral Sea            | 24 July<br>2015            | 10.98°S;<br>164.57°E              | <i>R/V<br/>Cassiopee</i> | Australian<br>Commonwealth<br>Scientific and<br>Industrial<br>Research<br>Organization<br>(CSIRO) | 148                                  |
| 2903005<br>2903327     | Northwest<br>Pacific | 3 February<br>2018         | 27.999°N;<br>165.003°E            | <i>R/V<br/>Keifumaru</i> | Japan Agency for<br>Marine-Earth<br>Science and<br>Technology<br>(JAMSTEC)                        | 61*<br>61*                           |

|         |                   |                    |                       |                                   |  |    |
|---------|-------------------|--------------------|-----------------------|-----------------------------------|--|----|
| 2902730 | Philippine<br>Sea | 11 January<br>2018 | 11.98°N;<br>129.998°E | <i>R/V Ke<br/>Xue San<br/>Hao</i> | China Second<br>Institute of<br>Oceanography<br>(CSIO) | 69 |
|---------|-------------------|--------------------|-----------------------|-----------------------------------|--|----|

576

577 \*During the starting two-month period, both Japan Argo floats operated at 1-day cycles and  
578 starting March 28, 2018 switched to 10-day cycles. To avoid overweighting of the starting period  
579 in the drift assessment, one of every 10 consecutive profiles was selected for both floats before  
580 March 28, 2018.

581 Table 2. Salinity offsets calculated by the OWC method at different reference datasets and time  
 582 separation factors. Numbers in bold indicate the reference dataset and time separation factors  
 583 selected for analysis.

584

| IFREMER<br>DMQC<br>reference dataset | Small/large<br>time separation<br>factors (years) | Argo<br>Australia<br>5904925 | Japan<br>Argo<br>2903005 | Japan<br>Argo<br>2903317 | China<br>Argo<br>2902730 |
|--------------------------------------|---|------------------------------|--------------------------|--------------------------|--------------------------|
| CTD 2019v01                          | 1/3   | -0.0152                      | -0.0116                  | -0.0139                  | -0.0139                  |
|                                      | 3/10  | -0.0167                      | -0.0088                  | -0.0107                  | -0.0144                  |
|                                      | 10/30   | -0.0152                      | -0.0077                  | -0.0075                  | -0.0076                  |
| Argo 2019v01                         | 1/3   | -0.0114                      | <b>-0.0009</b>           | <b>-0.0020</b>           | 0.0017                   |
|                                      | 3/10  | <b>-0.0100</b>               | -0.0065                  | -0.0037                  | <b>-0.0016</b>           |
|                                      | 10/30   | -0.0132                      | -0.0149                  | -0.0163                  | -0.0068                  |

585

586 Table 3. Assessment of the initial accuracy of the four Argo floats with RBR*argo* CTDs in the  
 587 Pacific Ocean compared to the CTD and Rosette profiles collected in parallel with the float  
 588 deployment, and the World Ocean Atlas data in the deployment locations. Numbers in bold  
 589 exceed the Argo accuracy requirements.

| Float                     | Distance (km) | Difference<br>in time<br>(h) | Salinity offset in the layer with potential<br>temperature 2–5°C; averaged difference<br>(Reference - Argo), calculated along potential<br>density levels |         |                             |
|---------------------------|---------------|------------------------------|---|---------|-----------------------------|
|                           |               |                              | bottle  | SBE911  | World Ocean Atlas<br>(WOA1) |
| Argo Australia<br>5904925 | 2.5           | 25.2                         | <b>-0.0114</b>  | -0.0081 | <b>-0.0124</b>              |
| Japan Argo<br>2903005     | 0.38          | 23.1                         | -0.0044   | -0.0034 | -0.0024                     |
| Japan Argo<br>2903317     | 0.30          | 23.7                         | -0.0090   | -0.0081 | -0.0066                     |
| China Argo<br>2902730     | 0.38          | 19.2                         | no data   | -0.0044 | -0.0006                     |

590

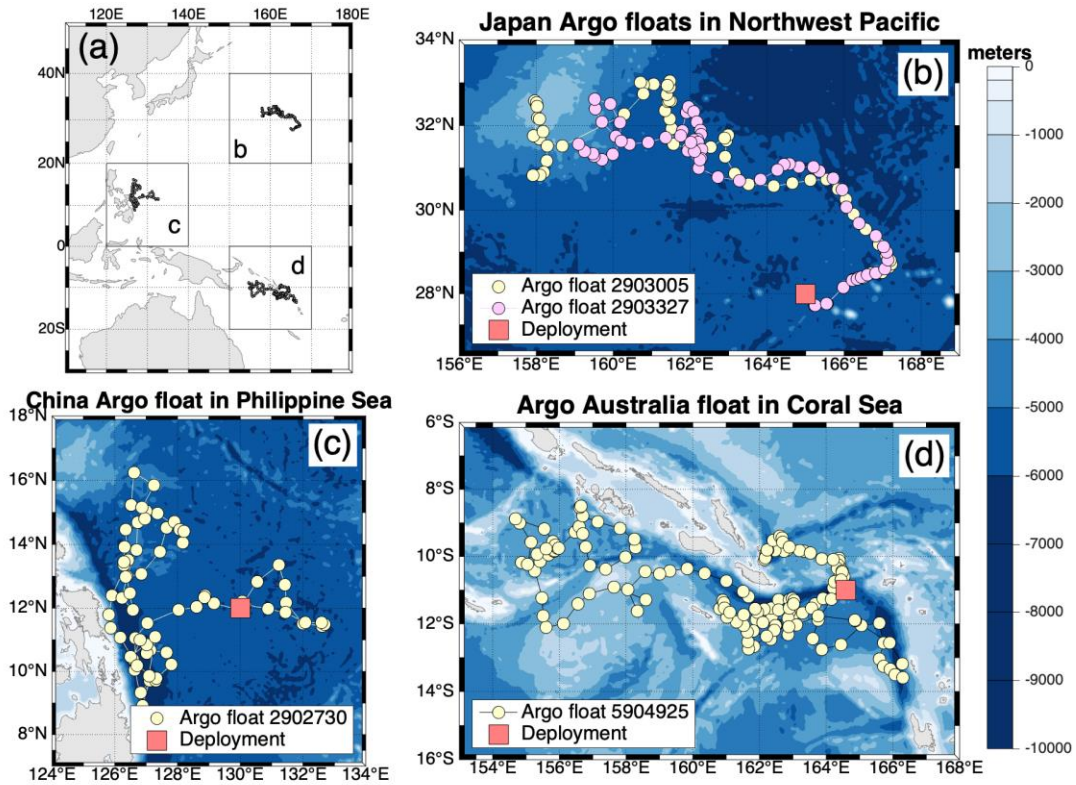
591

592 **Table A1. Parameters values used for OM interpolation (the file "ow\_config.txt") in OWC**  
 593 **analysis**

|   | <b>Parameter</b>   | <b>OWC variable</b>      | <b>Value</b>     |
|---|--|--------------------------|------------------|
| 1 | Maximum number of historical casts used in objective mapping | CONFIG_MAX_CASTS         | 300<br>(default) |
| 2 | Use/not use PV constraint                                    | MAP_USE_PV               | 0                |
| 3 | Use SAF separation criteria                                  | MAP_USE_SAF              | 0                |
| 4 | Spatial decorrelation scales (degrees)                       | MAPSCALE_LONGITUDE_LARGE | 4                |
|   |  | MAPSCALE_LONGITUDE_SMALL | 2                |
|   |  | MAPSCALE_LATITUDE_LARGE  | 4                |
|   |  | MAPSCALE_LATITUDE_SMALL  | 2                |
| 5 | Cross-isobath scales   | MAPSCALE_PHI_LARGE       | 0.5<br>(default) |
|   |  | MAPSCALE_PHI_SMALL       | 0.1<br>(default) |

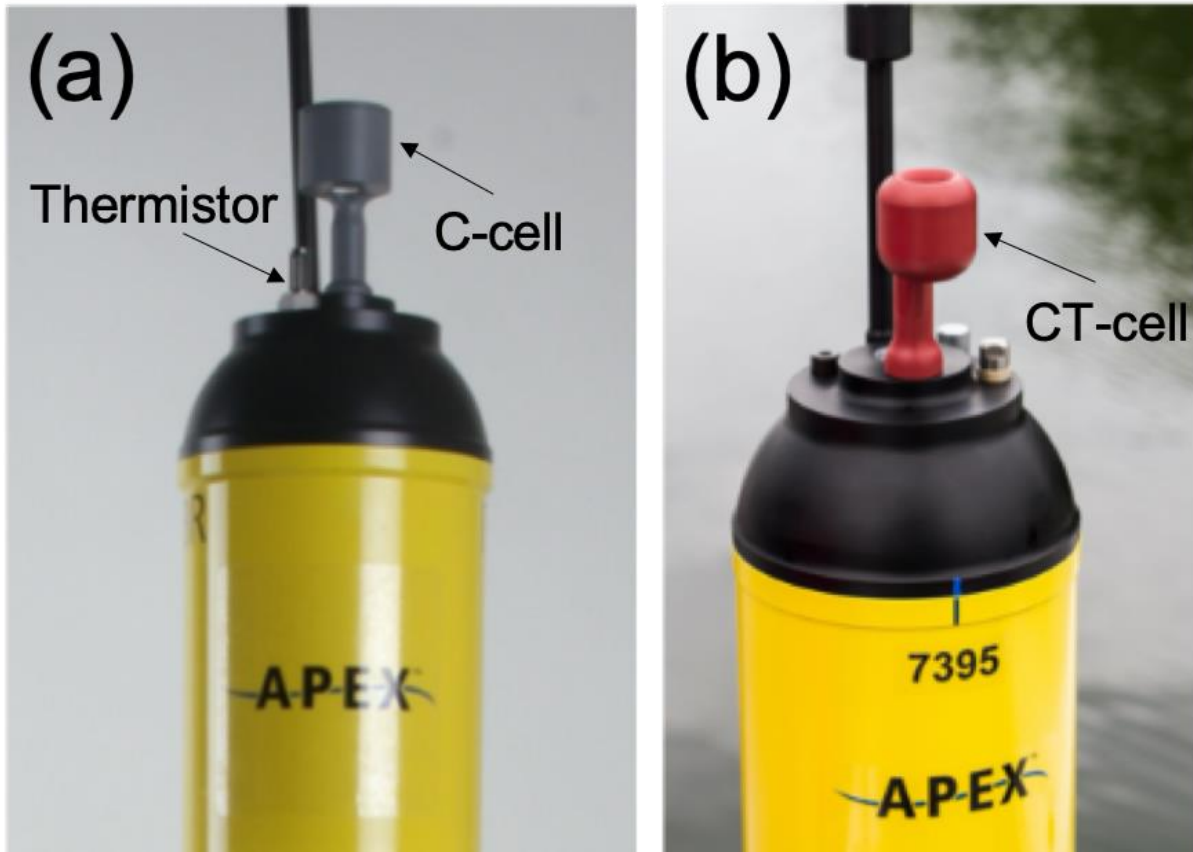
|   |   |  |  |
|---|---|--|--|
| 6 | Temporal decorrelation scale (years)                                  | MAPSCALE_AGE<br><br>MAPSCALE_AGE_LARGE | 1-10<br><br>3-30<br><br>see Section<br><br>3.1 |
| 7 | Exclude the top xxx dbar of the water column                          | MAP_P_EXCLUDE                          | 1000   |
| 8 | Only use historical data that are within +/- yyy dbar from float data | MAP_P_DELTA                            | 250<br><br>(default)                           |

594



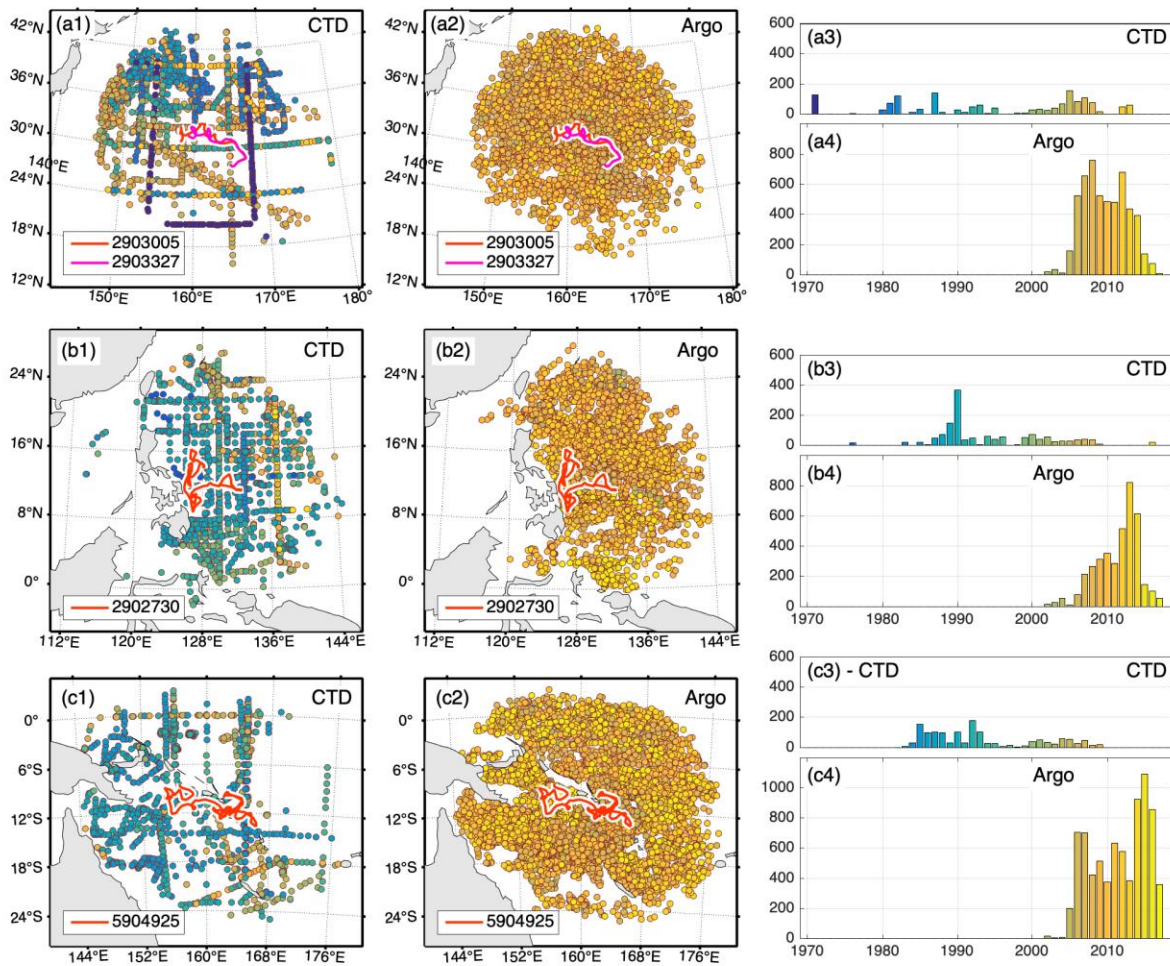
596

597 Figure 1. Four Argo floats equipped with RBRargo CTDs operating in the western Pacific  
 598 Ocean. Rectangles around each float in (a) indicate the regions where other Argo floats  
 599 (deployed starting January 2011) were selected for comparison (Section 3.3). Red squares in (b)–  
 600 (d) indicate the deployment locations where the CTD profiles used for assessment of the initial  
 601 accuracy of Argo salinity measurements (Section 3.2) were collected. The color shading in (b)–  
 602 (d) indicates bathymetry.



603

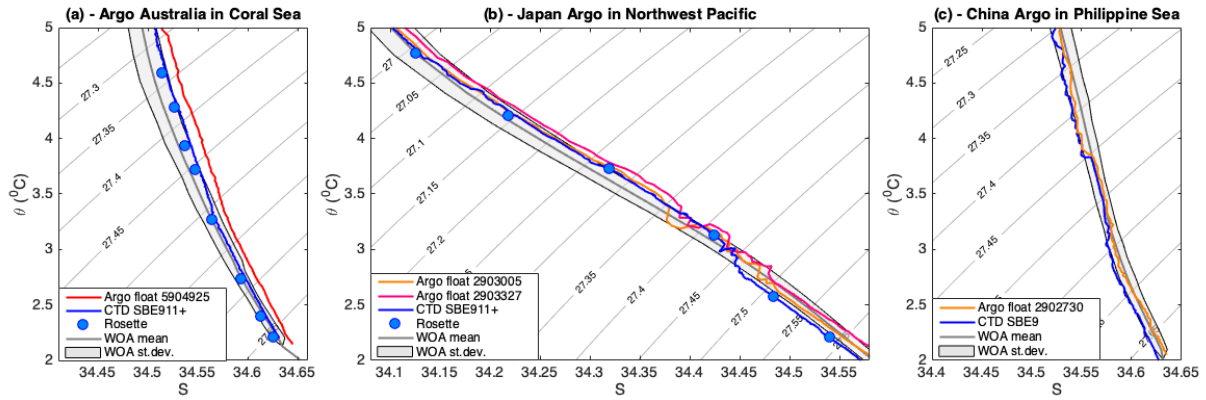
604 Figure 2. Photographs of (a) the RBR*argo* CTD with inductive conductivity cell (“C-cell”)  
605 (previous to 2016) and (b) the current inductive cell (“CT-cell”). The thermistor on the CT cell is  
606 collocated with the conductivity cell, however in the photo it is on the far side of the cell and  
607 therefore not visible. Photos courtesy of Teledyne Marine.



609

610 Figure 3. Availability of reference data for OWC analysis of RBRargo floats: Japan Argo (a1–  
 611 a4); China Argo (b1–b4) and Argo Australia (c1–c4); CTD casts (a1, a3, b1, b3, c1, c3) and  
 612 DMQC-corrected Argo profiles (a2, a4, b2, b4, c2, c4). Maps (a1, a2, b1, b2, c1, c2) demonstrate  
 613 the locations of reference data; histograms (a3, a4, b3, b4, c3, c4) demonstrate the numbers of  
 614 profiles collected during different years. The color scale in maps and histograms indicate the  
 615 years when reference data were collected.

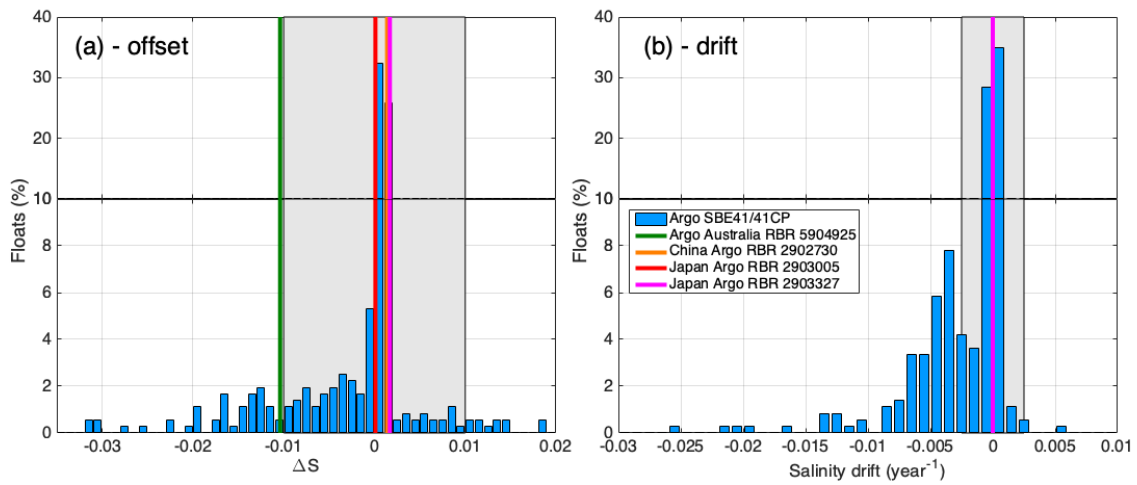
616



617

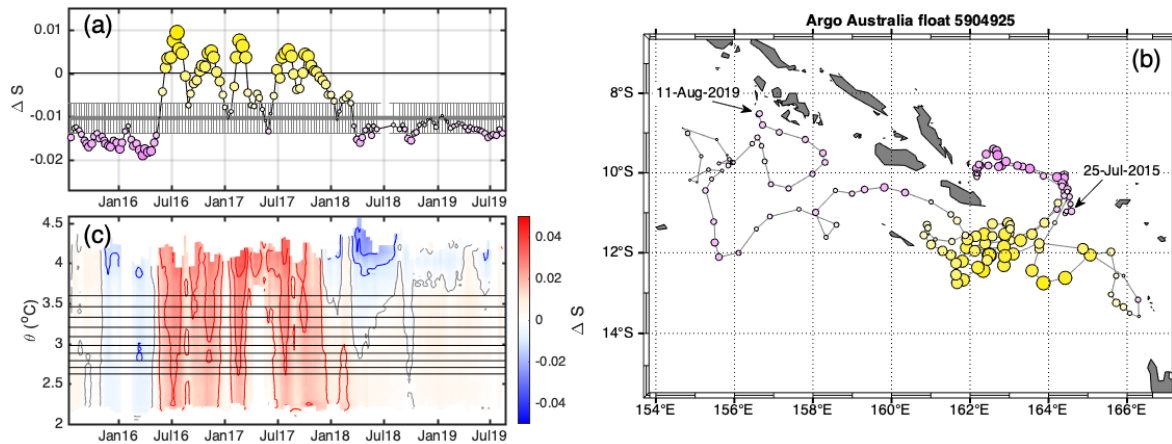
618 Figure 4. Comparison between the starting profiles of the four Argo floats equipped with  
 619 RBRargo CTDs, CTD casts collected when the float was deployed, and the World Ocean Atlas  
 620 (WOA1) climatological data at the deployment locations. X-axes are practical salinity; Y-axes  
 621 are potential temperature ( $^{\circ}\text{C}$ ).

622



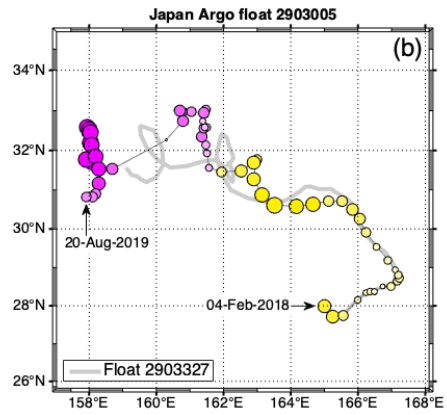
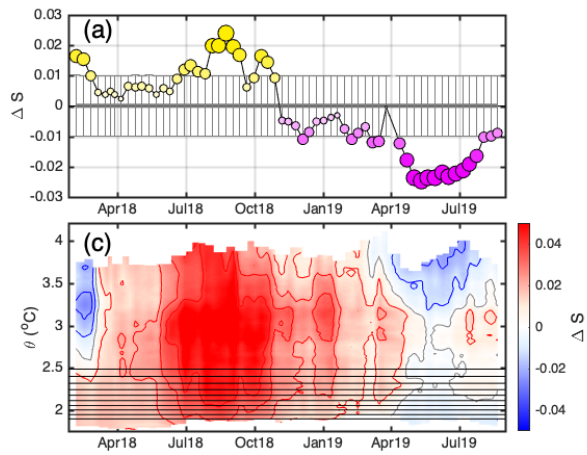
623

624 Figure 5. The averaged salinity (a) correction bias and (b) drift (the slope of the linear change of  
 625 the correction offset between the beginning and the end of the float lifetime) in four Argo floats  
 626 with RBR<sub>argo</sub> CTDs and 360 Argo floats with electrode conductivity sensors operating in the  
 627 same areas since 2011 (blue bars). Shaded areas show: (a) the target accuracy of Argo salinity  
 628 measurements (0.01) and (b) the stability limits of Argo salinity measurements (0.01 in 4 years =  
 629 0.0025 year<sup>-1</sup>). Note that in (b) the drift estimates for all four RBR<sub>argo</sub> CTDs indicated in the  
 630 legend are zero.



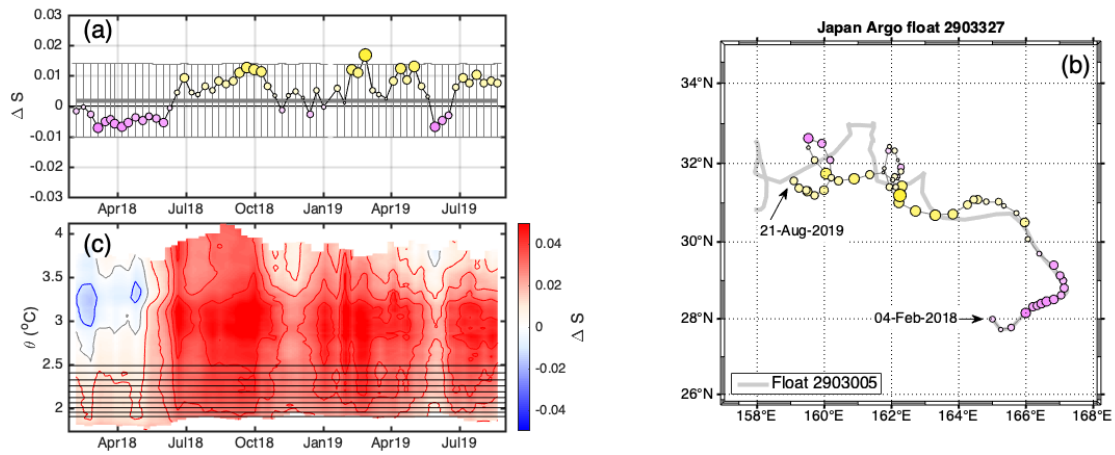
631

632 Figure 6. (a) OWC profile fit coefficients for Argo Australia float 5904925, (b) geographical  
 633 location of the profiles with different OWC fit coefficients. The size and color of the circles  
 634 indicate the deviations of the profile fit coefficients from the constant offset. Arrows with dates  
 635 indicate the start and end float positions. (c) The differences between the reference salinity  
 636 calculated by the OWC method using the Argo reference database and the World Ocean Atlas  
 637 (2005-2017) climatology (Y-scale is potential temperature). Horizontal lines in (c) show the 10  
 638 potential temperature levels with minimum salinity variations used for the OWC analysis.



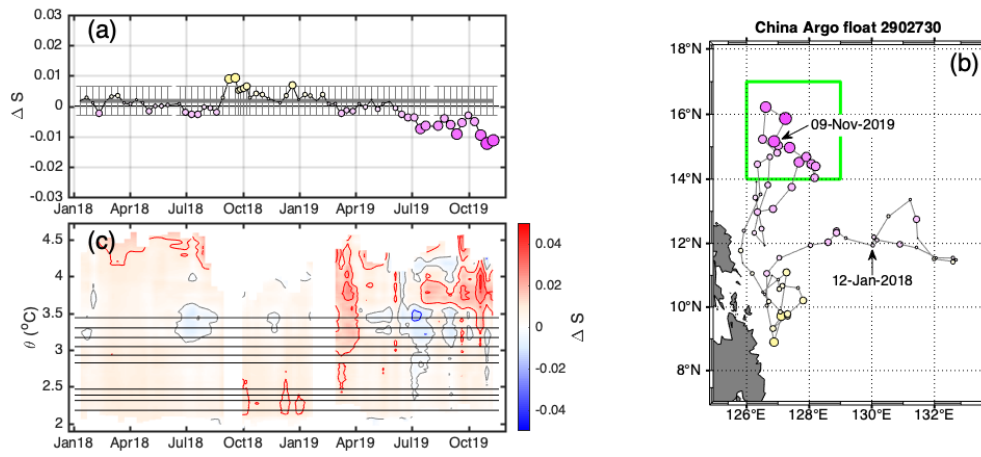
639

640 Figure 7. Similar to Figure 6, for Japan Argo float 2903005. Gray line in (b) shows the trajectory  
 641 of the Japan Argo float 2903327 deployed in parallel with the float 2903005.



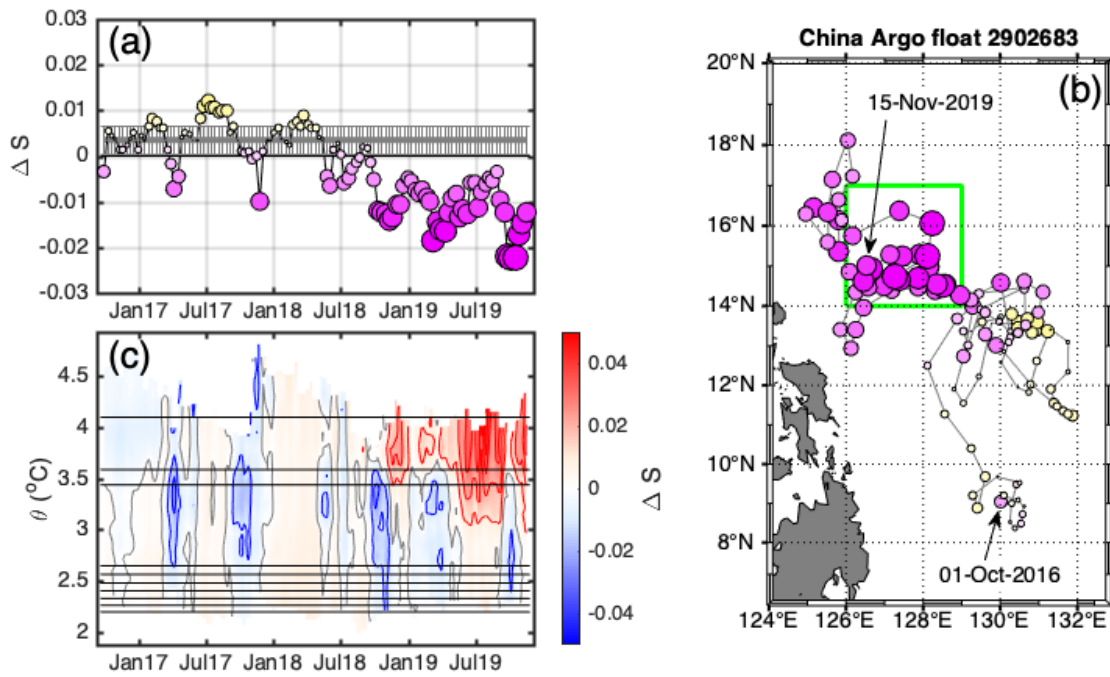
642

643 Figure 8. Similar to Figures 6–7, for Japan Argo float 2903327. Gray line in (b) shows the  
 644 trajectory of Japan Argo float 2903005 deployed in parallel with the float 2903327.



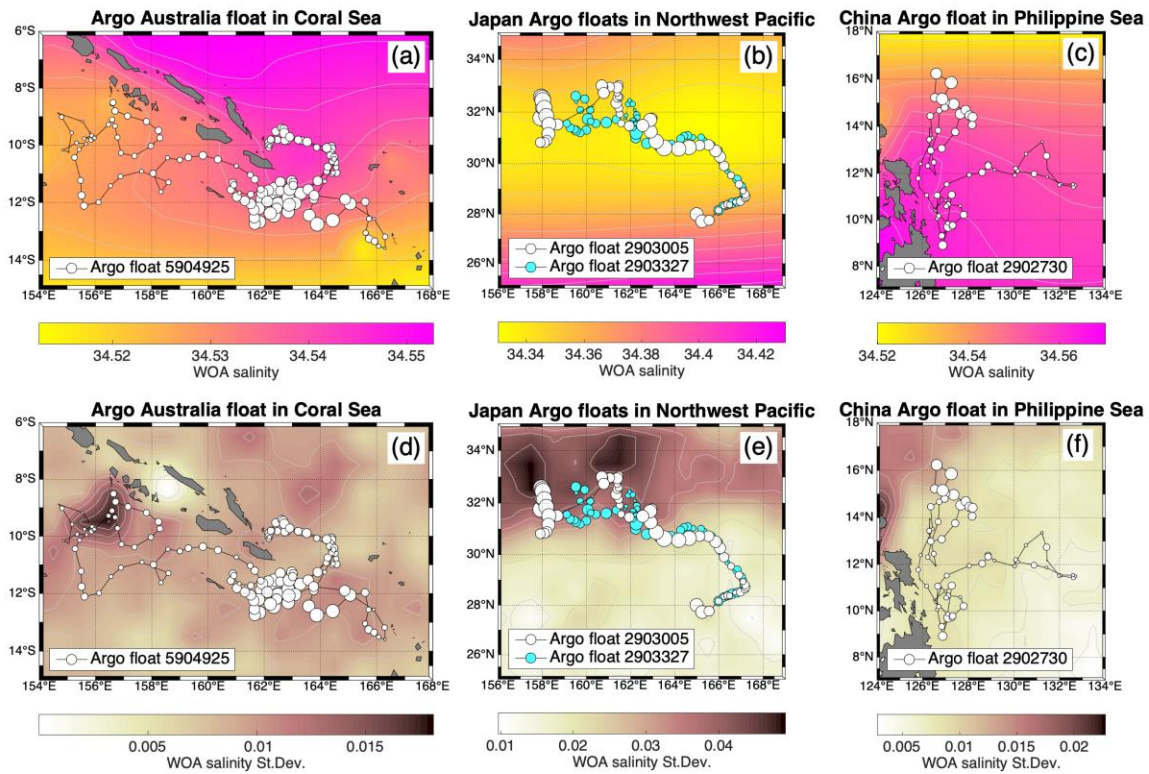
645

646 Figure 9. Similar to Figures 6–8, for China Argo float 2902730.



647

648 Figure 10. Similar to Figures 6–9, for China Argo float 2902683 with SBE41 CTD operating in  
 649 the same area and the same time with the China Argo float 2902730 (Figure 9).



650

651 Figure 11. World Ocean Atlas [Garcia et al., 2018] salinity means (a-c) and standard deviations  
 652 (d-f) averaged in the 1000–1200 dbar layer in (a, d) the Coral Sea, (b, e) the Northwest Pacific  
 653 and (c, f) the Philippine Sea, where the Argo floats with RBRargo CTDs operated. The size of  
 654 circles along the float trajectories is proportional to the differences between the profile fit  
 655 coefficients and the mean offsets calculated by the OWC method (similar to Figures 6b-9b).

656